

Iron Complexes with the Alcoholato Donor-Rich Ligand 4-*tert*-Butyl-2,6-bis(hydroxymethyl)phenol: Synthesis and Characterization of a Tetra-Anionic Fe₂ Complex and a Neutral Fe₁₀Na₄ Complex

Thorsten Glaser,^{*,[a]} Thomas Lügger,^[a] and Rolf-Dieter Hoffmann^[a]

Keywords: Iron / O ligands / Oxo ligands / Bridging ligands / Hydrogen bonds

The reaction of 4-*tert*-butyl-2,6-bis(hydroxymethyl)phenol (H₃L) with Fe^{III} ions in methanol in the presence of an excess of NaOH afforded the tetra-anionic dinuclear complex Na₄[(HL)₄Fe^{III}₂(CO₃)]·11MeOH·3H₂O (**1**). Changing the solvent to an ethanol/dme (dme = 1,2-dimethoxyethane) mixture led to the formation of the decanuclear complex [(HL)₁₂Fe^{III}₁₀Na₄(μ₄-O)₄(μ₃-OH)₂(dme)₂(EtOH)₂]·2dme·8EtOH (**2**). The Mössbauer spectra of **1**' and **2** at 80 K are consistent with high spin Fe^{III} sites in distorted octahedral O₆ coordination environments. Compound **1** consists of a tetra-anionic dinuclear iron complex with the unprecedented [Fe^{III}(μ₂-

OBz)₂(μ₂-CO₃)Fe^{III}]²⁺ core. Compound **2** contains a core of hydrous ferric oxide produced by a modified hydrolysis of Fe^{III} ions in the presence of the ligand. Eight benzyl alcohol groups are located on the surface of **2** leading to a 2D network structure by intermolecular hydrogen bonding. The temperature dependence of the magnetic susceptibilities of **1**' and **2** indicates antiferromagnetic interactions between the ferric ions. The data for **1**' were fitted with $J = -4.4 \text{ cm}^{-1}$ and $g = 1.98$, $H = -2JS_1S_2$.

(© Wiley-VCH Verlag GmbH & Co. KGaA, 69451 Weinheim, Germany, 2004)

Introduction

Polynuclear oxo-, hydroxo-, and alcoholato-bridged iron complexes have received a great deal of attention in the fields of bioinorganic chemistry and molecular magnetic materials. In the former, they have been discussed as models for the high-nuclearity hydrous ferric oxide core of the iron storage protein ferritin.^[1] Additionally, high-nuclearity iron complexes with high spin ground states and large negative magnetic anisotropy can behave as single-molecule magnets (SMMs).^[2] A number of polynuclear complexes with a non-wheel-like structure comprised of up to 19 iron centers are known.^[3] Joining together such aggregates into 1D, 2D, or 3D assemblies can yield materials with interesting magnetic properties.^[4]

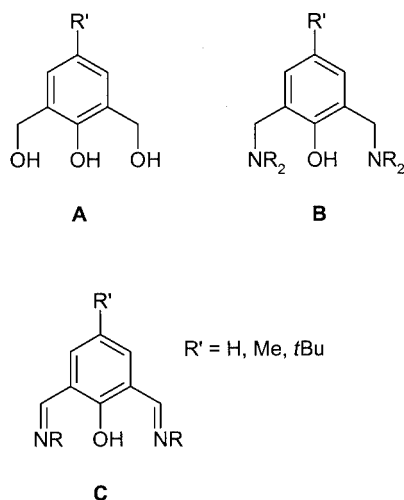
In this respect, we have been exploring the coordination chemistry of ligands based on 2,6-bis(hydroxymethyl)phenol **A** (Scheme 1) and the sulfur-substituted derivatives, which are of particular interest due to the number of possible binding modes that they may display. Although the coordination chemistry of the corresponding ligand types 2,6-bis(aminomethyl)phenol **B** and 2,6-bis(iminomethyl)phenol **C** (dinucleating ligands or Robson type ligands)^[5] is well established, neither the coordination chemistry of the

benzyl alcohol ligand **A**,^[6] nor the coordination chemistry of benzyl alcohol ligands in general is well established. One important property of alcoholato ligands is their strong basicity, mainly due to the lack of resonance stabilization of the corresponding anion. This leads to their pronounced tendency to bridge metal centers^[7] rather than to bind to one metal center in a terminal fashion, which is the usual coordination mode of amine and imine nitrogen donors. The coordination chemistry of ligand types **B** and **C** is, therefore, dominated by dinuclear metal complexes whereas ligand type **A** is well suited for the preparation of a variety of high-nuclearity complexes with differing coordination modes.^[8] The related ligand 2,6-bis(hydroxymethyl)pyridine has been used for the synthesis of polynuclear manganese complexes, which exhibit single-molecule magnetic behavior.^[9]

Recently, we reported that the reaction of 4-*tert*-butyl-2,6-bis(hydroxymethyl)phenol (H₃L) with [Fe^{III}(acac)₃] in CH₃CN in the presence of Et₃N yields the tetranuclear complex (Et₃NH)₂[(HL)₆Fe^{III}₄(acac)₂] (**3**) with a core of two face-sharing cuboidal [Fe₃O₄] fragments.^[6a] The central phenolato donor (OPh⁻) in each of the three crystallographically independent ligand molecules coordinates in a terminal fashion to one Fe ion. The two benzyl alcohol groups of each ligand are distinguishable. One benzyl alcohol group of each ligand is deprotonated (OBz⁻) while the other one is not (BzOH). The deprotonated benzyl alcoholato donors coordinate either in a μ₂- or in a μ₃-bridging mode. The protonated, non-coordinating benzyl alcohol groups form intra- as well as intermolecular hydrogen

^[a] Institut für Anorganische und Analytische Chemie, Westfälische Wilhelms-Universität Münster, Wilhelm-Klemm-Straße 8, 48149 Münster, Germany
Fax: (internat) +49-(0)251 833 3108
E-mail: tglaser@uni-muenster.de

Supporting information for this article is available on the WWW under <http://www.eurjic.org> or from the author.



Scheme 1

bonds. In this way, the zero-dimensional paramagnetic building block was arranged into a 1D array by hydrogen bonding. Here, we report on the reaction between H₃L and Fe^{III}(ClO₄)₃·10H₂O in the presence of NaOH in protic solvents. Using MeOH as the solvent led to a tetra-anionic dinuclear iron complex and using an EtOH/dme mixture (dme = 1,2-dimethoxyethane) led to a decanuclear complex which forms a 2D network structure in the solid state by intermolecular hydrogen bonds.

Results and Analysis

Synthesis and Structural Characterization

The reaction between H₃L and Fe^{III}(ClO₄)₃·10H₂O in a 2:1 molar ratio in methanol in the presence of excess NaOH per ligand yielded large red crystals of **1** which were isolated by filtration. The FTIR spectrum exhibits bands at 2954, 2868, 1480, 1392 and 1363 cm⁻¹ that are characteristic of the *tert*-butylbenzene section of the ligand H₃L. The C–O stretching frequencies of the phenolic C–O bonds are at 1307, 1276, and 1219 cm⁻¹ compared with 1219 cm⁻¹ in the free ligand H₃L.^[6a,10] The broad band of the benzylic C–O bond at 1015 cm⁻¹ in the free ligand splits into two sharp bands at 1039 and 1021 cm⁻¹ in **1**. A broad flat absorption in the range of 2500–3500 cm⁻¹ indicates the occurrence of hydrogen bonds. Red crystals of **1** were investigated by means of a single-crystal X-ray diffraction study and a composition of Na₄[(HL)₄Fe₂(CO₃)]·11MeOH·3H₂O was obtained. Samples used for magnetic measurements were dried under high vacuum and analysis revealed a composition of Na₄[(HL)₄Fe₂(CO₃)]·8MeOH·2H₂O (**1'**) indicating the loss of 3 MeOH molecules and one H₂O molecule. Tetra-anionic dinuclear complexes [(HL)₄Fe₂(CO₃)]⁴⁻ (Figure 1) are bridged in one direction by a complicated and disordered network of sodium cations, methanol and water molecules. Although the dinuclear complex could be refined well, the heavily disordered Na⁺ cations and methanol and

water molecules (≈ 35% of total scattering power) have precluded complete refinement. Therefore, we have used the results from the X-ray diffraction analysis as proof only of atomic connectivity.^[11]

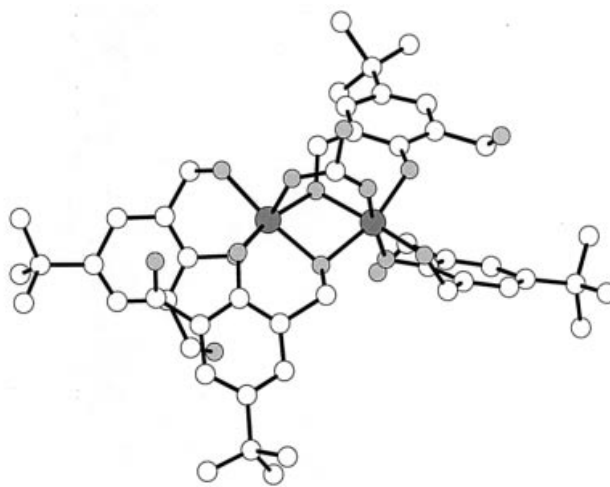


Figure 1. Atomic connectivity in the dinuclear complex [(LH)₄Fe₂(CO₃)]⁴⁻ in **1**; dark grey circles: Fe; light grey circles: O; empty circles: C

Due to the lack of added carbonate, CO₃²⁻, or hydrogen carbonate, HCO₃⁻, the incorporated carbonato ligand has to originate from atmospheric CO₂. To test this hypothesis, we performed the same reaction under an argon atmosphere and no pure product was obtained. In other attempts to obtain **1** in a more controlled fashion Na₂CO₃, a typical precursor for the preparation of iron-carbonato complexes,^[12] was added to the reaction mixture. However, no pure product was obtained. Although the controlled reaction for the preparation of **1** proved not to be straightforward, the reaction under a normal atmosphere was repeated several times and large red crystals were obtained in each case. It is interesting to note that analogous reactions using LiOH, KOH, CsOH, or even *t*BuOK and Et₃N as bases did not yield the tetra-anion of **1**. It might be speculated, therefore, that there is a synergistic effect of CO₂ incorporation and the incorporation of Na⁺ ions in the solid state. Fixation of CO₂ under the highly basic conditions used in our preparations is not surprising, and this has been studied in detail by Kitajima et al.^[13]

The potentially tridentate ligand is only doubly deprotonated i.e. HL²⁻. In two ligand molecules, the phenolato group acts as a terminal donor, whereas the deprotonated benzyl alcoholato donor acts as a μ₂-bridge between the iron ions. The non-deprotonated benzyl alcohol functions form hydrogen bonds with the coordinated phenolato oxygens and with methanol molecules. In the other two ligands, the phenolato oxygen atom and the deprotonated benzyl alcohol oxygen atom chelate an iron atom whereas the non-deprotonated benzyl alcohol group binds to two sodium ions. The dinuclear complex is composed of a central [Fe^{III}(μ₂-OBz)₂Fe^{III}]⁴⁺ core which represents a fundamental unit in iron-oxygen donor chemistry of metallo-pro-

teins and of biomimetic model compounds.^[14] Several examples of complexes with the $[\text{Fe}^{\text{III}}(\mu_2\text{-OR})_2(\mu_2\text{-OOCR}')\text{Fe}^{\text{III}}]^{3+}$ core have been reported.^[15] Whereas $[\text{Fe}^{\text{III}}(\mu_2\text{-O})(\mu_2\text{-CO}_3)\text{Fe}^{\text{III}}]^{2+}$ is known^[12,13], however, complex **1** is to the best of our knowledge the first evidence of a $[\text{Fe}^{\text{III}}(\mu_2\text{-OR})_2(\mu_2\text{-CO}_3)\text{Fe}^{\text{III}}]^{2+}$ core.

The reaction of H_3L and $\text{Fe}^{\text{III}}(\text{ClO}_4)_3 \cdot 10\text{H}_2\text{O}$ in a molar ratio of 2:1 in ethanol in the presence of excess NaOH and dme yielded dark red crystals of **2**. The FTIR spectrum shows the bands of the *tert*-butylbenzene part of the ligand H_3L at 2954, 2867, 1480, 1393, and 1363 cm^{-1} . The absorptions at 1306, 1275, and 1220 cm^{-1} can be assigned to C–O stretching modes of the phenolic C–O bonds, and those at 1038 and 1022 cm^{-1} to the C–O stretching modes of the benzylic C–O bonds. The intensity patterns of these C–O vibrations differ from those observed in the FTIR spectrum of **1**. A broad flat absorption in the 3400–2500 cm^{-1} range is indicative of hydrogen bonding. Structural characterization by single-crystal X-ray diffraction gave the formulation as $[(\text{HL})_{12}\text{Fe}^{\text{III}}_{10}\text{Na}_4(\mu_4\text{-O})_4(\mu_3\text{-OH})_2(\text{dme})_2(\text{EtOH})_2] \cdot 2\text{dme} \cdot 8\text{EtOH}$ (**2**).

The molecular structure of the decanuclear complex in crystals of **2** is shown in Figure 2 (a). The decanuclear iron unit including the bridging oxygen atoms is shown in Figure (b). Selected bond lengths and bond angles are given in Table 1. The asymmetric unit consists of one half of the complex with the other half generated by a crystallographic center of inversion. All iron atoms are in distorted octahedral FeO_6 environments and are bridged by four $\mu_4\text{-O}^{2-}$ (O1 , $\text{O1}'$, O3 , $\text{O3}'$), two $\mu_3\text{-OH}^-$ (O3 , $\text{O3}'$), and twelve $\mu_2\text{-OBz}^-$ ligands (O2a , $\text{O2a}'$, O2b , $\text{O2b}'$, O2c , $\text{O2c}'$, O2d , $\text{O2d}'$, O2e , $\text{O2e}'$, O2f , $\text{O2f}'$). The coordination of the iron ions is completed by OPh^- ligands and two EtOH ligands (coordinated to Fe3 and $\text{Fe3}'$). The assignment of O2 (and $\text{O2}'$) to an OH^- instead of an O^{2-} ligand is not only based on charge considerations. The three Fe–O bond lengths to O2 (mean value 2.09 Å) are significantly longer than the four bond lengths to O1 (2.02 Å) and O3 (2.05 Å). For O2 being a $\mu_3\text{-O}^{2-}$, it must have shorter bonds compared with a $\mu_4\text{-O}^{2-}$. Additionally, one oxygen of dme adopts the fourth position of an idealized tetrahedron around O2 at a distance of 2.77 Å, consistent with a hydrogen bond (see Figure S1 in the Supporting Information, for Supporting Information see also the footnote on the first page of this article). The Fe–O bond lengths span a range from 1.95 Å to 2.12 Å. A comparison of the bridging ligands shows that the $\mu_2\text{-OBz}^-$ ligands have shorter bonds (mean value 2.00 Å) compared with the $\mu_4\text{-O}^{2-}$ (mean value 2.03 Å) and the $\mu_3\text{-OH}^-$ ligands (mean value 2.09 Å). The Fe···Fe distances can be divided into two categories: a short distance was found for $\text{Fe1}\text{--}\text{Fe1}'$, $\text{Fe1}\text{--}\text{Fe2}'$, and $\text{Fe2}\text{--}\text{Fe1}'$ at 3.00–3.02 Å and a significantly longer distance range of 3.10–3.22 Å for all other Fe···Fe separations.

The iron-oxygen core can be regarded as a part of a hydrous ferric oxide phase. The oxygen atoms of the bridging $\mu_4\text{-O}^{2-}$, $\mu_3\text{-OH}^-$, $\mu_2\text{-OBz}^-$, and the terminal OPh^- and EtOH may be considered to form an idealized cubic close packed structure with the iron atoms in octahedral voids (A

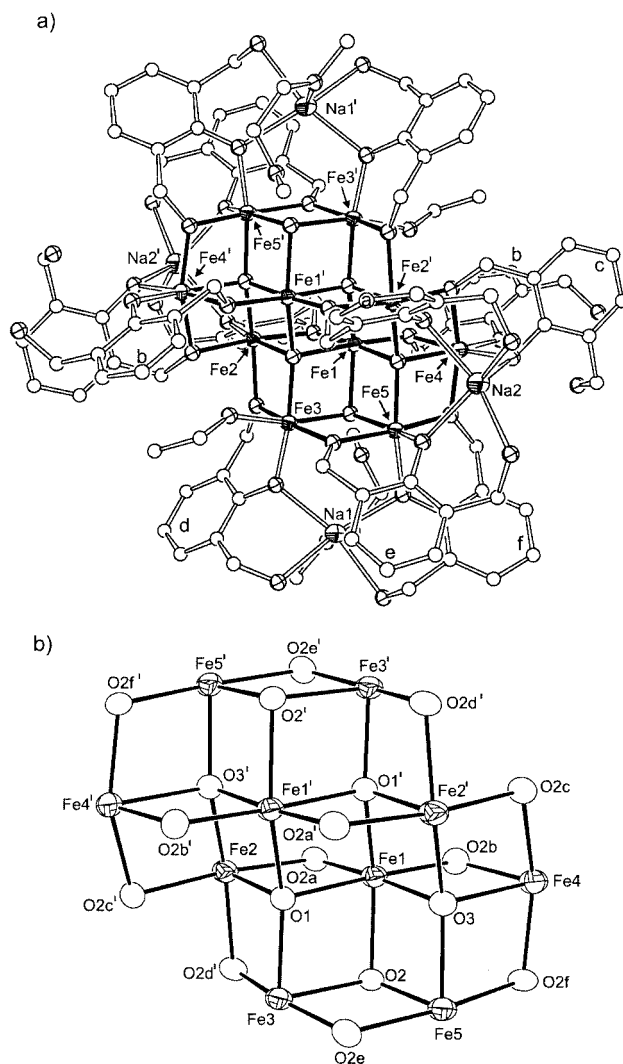


Figure 2. a) Molecular structure of $[(\text{HL})_{12}\text{Fe}^{\text{III}}_{10}\text{Na}_4(\mu_4\text{-O})_4(\mu_3\text{-OH})_2(\text{dme})_2(\text{EtOH})_2]$ in crystals of **2**; hydrogen atoms and *tert*-butyl groups are omitted for clarity. The six independent ligand molecules are labeled a–f; b) ORTEP plot of the central Fe_{10} core including the bridging oxygen atoms; thermal ellipsoids are shown at the 50% probability level

B C A B stacking sequence, see Figure S2 in the Supporting Information). In this respect, the iron-oxygen core in **2** may be regarded as a small part of $\gamma\text{-Fe}_2\text{O}_3$ or lepidocrocite stabilized by an organic shell. Two Fe_{10} complexes with a similar iron-oxygen core were reported, namely $[\text{Fe}_{10}\text{O}_4(\text{OCH}_3)_{16}(\text{dbm})_6] \cdot x\text{CHCl}_3$ ($\text{Hdbm} = 1,3\text{-diphenyl-1,3-propanedione}$)^[3e] and $[\text{Fe}_{10}\text{O}_4\text{Cl}_8(\text{OCH}_3)_{14}(\text{CH}_3\text{OH})_6] \cdot 2\text{CH}_3\text{OH}$.^[3f] This indicates a high stability of the iron-oxygen core based on the different kind of outer shell ligands used for the preparation of the three compounds.

The potentially tridentate ligand H_3L appears in all six independent ligand molecules (labeled a–f in Figure 2, a) as only doubly deprotonated HL^{2-} . One of the BzOH groups of each ligand is not deprotonated ($\text{O3a}\text{--}\text{O3f}$). The six ligand molecules coordinate in two different binding modes. Ligand b (O1b , O2b , O3b) and ligand c (O1c , O2c ,

Table 1. Selected interatomic distances (Å) and bond angles (°) for **2**

Fe1–O1 (μ ₄ -O)	2.062(4)	Fe1–Fe3	3.131(1)
Fe1–O1' (μ ₄ -O)	1.950(4)	Fe1–Fe4	3.165(2)
Fe1–O3 (μ ₄ -O)	2.066(4)	Fe1–Fe5	3.161(1)
Fe1–O2 (μ ₃ -OH)	2.083(4)	Fe2–Fe1'	2.993(2)
Fe1–O2a (μ ₂ -OBz)	1.974(4)	Fe2–Fe3	3.098(2)
Fe1–O2b (μ ₂ -OBz)	1.944(4)	Fe2–Fe4'	3.153(1)
Fe2–O1 (μ ₄ -O)	2.089(4)	Fe3–Fe5	3.214(2)
Fe2–O3' (μ ₄ -O)	1.964(4)	Fe4–Fe2'	3.153(1)
Fe2–O2a (μ ₂ -OBz)	2.029(4)	Fe4–Fe5	3.170(2)
Fe2–O2c' (μ ₂ -OBz)	2.108(4)	Fe1–O1(μ ₄ -O)–Fe1'	97.6(2)
Fe2–O2d (μ ₂ -OBz)	2.013(4)	Fe1–O1'(μ ₄ -O)–Fe1'	97.6(2)
Fe2–O1a (μ ₂ -OPh)	1.909(4)	Fe1–O1(μ ₄ -O)–Fe2	97.2(2)
Fe3–O1 (μ ₄ -O)	1.972(4)	Fe1–O2a(μ ₂ -OBz)–Fe2	102.2(2)
Fe3–O2 (μ ₃ -OH)	2.083(4)	Fe1–O1'(μ ₄ -O)–Fe2'	95.6(2)
Fe3–O2d (μ ₂ -OBz)	1.978(4)	Fe1–O3(μ ₄ -O)–Fe2'	95.9(2)
Fe3–O2e (μ ₂ -OBz)	1.975(4)	Fe1–O1(μ ₄ -O)–Fe3	101.8(2)
Fe3–O1d (μ ₂ -OPh)	1.919(4)	Fe1–O2(μ ₃ -OH)–Fe3	97.5(2)
Fe3–O30 (HOEt)	2.095(4)	Fe1–O2b(μ ₂ -OBz)–Fe4	104.2(2)
Fe4–O3 (μ ₄ -O)	2.137(4)	Fe1–O3(μ ₄ -O)–Fe4	97.7(2)
Fe4–O2b (μ ₂ -OBz)	2.065(4)	Fe1–O2(μ ₃ -OH)–Fe5	97.7(2)
Fe4–O2c (μ ₂ -OBz)	2.009(4)	Fe1–O3(μ ₄ -O)–Fe5	101.1(2)
Fe4–O2f (μ ₂ -OBz)	1.946(4)	Fe2–O1(μ ₄ -O)–Fe1'	95.6(2)
Fe4–O1b (OPh)	1.970(4)	Fe2–O3'(μ ₄ -O)–Fe1'	95.9(2)
Fe4–O1c (OPh)	1.973(5)	Fe2–O1(μ ₄ -O)–Fe3	99.4(2)
Fe5–O3 (μ ₄ -O)	2.029(4)	Fe2–O2d(μ ₂ -OBz)–Fe3	101.8(2)
Fe5–O2 (μ ₃ -OH)	2.113(4)	Fe2–O2c'(μ ₂ -OBz)–Fe4'	100.0(2)
Fe5–O2e (μ ₂ -OBz)	2.003(4)	Fe2–O3'(μ ₄ -O)–Fe4'	100.4(2)
Fe5–O2f (μ ₂ -OBz)	1.989(4)	Fe3–O2(μ ₃ -OH)–Fe5	100.0(2)
Fe5–O1e (μ ₂ -OPh)	1.945(5)	Fe3–O2e(μ ₂ -OBz)–Fe5	107.7(2)
Fe5–O1f (μ ₂ -OPh)	2.020(4)	Fe4–O2c(μ ₂ -OBz)–Fe2'	100.0(2)
Fe1–Fe1'	3.020(2)	Fe4–O3(μ ₄ -O)–Fe2'	100.4(2)
Fe1–Fe2	3.115(2)	Fe4–O2f(μ ₂ -OBz)–Fe5	107.3(2)
Fe1–Fe2'	2.993(2)	Fe4–O3(μ ₄ -O)–Fe5	99.1(2)

O3c) bind only in a chelating fashion to the iron centers via the OPh[−] (O1b, O1c) and OBz[−] (O2b, O2c) groups, and OBz[−] bridges two iron centers. The second non-deprotonated BzOH (O3b, O3c) of these two ligands is not coordinated to a metal center. Ligands a, d, e, f chelate additionally to a Na⁺ ion via the OPh[−] group and the non-deprotonated BzOH. Furthermore, the non-deprotonated BzOH groups are involved in intra- and intermolecular hydrogen bonding. O3b and O3c (O3b' and O3c') form an intramolecular hydrogen bond with a distance of 2.79 Å. Intermolecular hydrogen bonds between O3f and O3b (2.68 Å) and between O3c and O3d (2.76 Å) lead to a hydrogen bonded 2D network structure in the *bc*-plane (Figure 3).

Spectroscopic Characterization

The ⁵⁷Fe Mössbauer spectrum of **1'** at 80 K shows a quadrupole doublet with an isomer shift $\delta = 0.47 \text{ mm}\cdot\text{s}^{-1}$ and a quadrupole splitting $|\Delta E_Q| = 0.69 \text{ mm}\cdot\text{s}^{-1}$. The isomer shift is typical for high-spin ferric ions ($S_i = 5/2$) ligated by oxygen donors. The quadrupole splitting of $0.69 \text{ mm}\cdot\text{s}^{-1}$ is consistent with a moderate distortion from octahedral symmetry since the valence-electron contribution to ΔE_Q is negligible for a high-spin Fe^{III} ion. The effective magnetic moment (μ_{eff} , calculated per iron dimer unit) of **1'** decreases with decreasing temperature which is indicative of antiferro-

magnetic coupling (Figure 4). The data could be easily fitted using the spin-Hamiltonian for an Fe^{III} ($S_i = 5/2$) dimer

$$H = -2JS_1S_2 + \sum_{i=1}^2 [\mu_B g_i S_i \mathbf{B}]$$

using a full-matrix diagonalization approach with $J = -4.4 \text{ cm}^{-1}$ and an isotropic g value of 1.98 including a paramagnetic impurity ($S = 5/2$) of 4.1%.^[16]

The Mössbauer spectrum of **2** at 80 K exhibits a well resolved doublet with $\delta = 0.51 \text{ mm}\cdot\text{s}^{-1}$ and $|\Delta E_Q| = 0.73 \text{ mm}\cdot\text{s}^{-1}$ typical for high-spin ferric ions. The subspectra originating from the five distinctive iron ions in **2** were not resolved. The temperature dependence of μ_{eff} indicates antiferromagnetic interactions between the Fe^{III} ions. At low temperatures, the μ_{eff} values appear to be sample-dependent. This may be due to different amounts of paramagnetic impurities (presumably mononuclear Fe^{III} species) or to sample inhomogeneities. Crystals rapidly lose solvent leading to different mixtures of crystalline (Fe₁₀Na₄·2dme·8EtOH) and amorphous parts (Fe₁₀Na₄·*x*dme·*x*EtOH) with loss of the regular hydrogen bonding pattern as observed in crystals of Fe₁₀Na₄·2dme·8EtOH. The change in the chemical environment of the formerly hydrogen bonded BzOH groups may have a direct effect on the bridges between the iron centers and thus on the exchange interactions leading to the observed differences in the magnetic measurements.

Discussion

The reaction of H₃L with Fe^{III}(ClO₄)₃·10H₂O in the presence of NaOH resulted in the formation of **1** using MeOH as the solvent, and **2** using an EtOH/dme mixture as the solvent. Complex **1** has an [Fe^{III}(μ₂-OBz)₂(μ₂-CO₃)Fe^{III}]²⁺ core which, to the best of our knowledge, is the first example of an Fe₂O₂ unit bridged by a carbonate ligand. The exchange coupling constant was found to be $J = -4.4 \text{ cm}^{-1}$. Analogous complexes with a carboxylato instead of the carbonate bridge, i.e. [Fe^{III}(μ₂-OR)₂(μ₂-O₂CR)Fe^{III}]³⁺, were reported to have J values in the range of -3.9 to -10.5 cm^{-1} .^[15c,15d,15e]

Uncoordinated benzyl alcohol groups, coordinated phenolato groups, and the uncoordinated oxygen atom of the coordinated carbonate ligand in **1** create an oxygen donor rich, negatively charged environment around the central [(HL)₄Fe₂(CO₃)]^{4−} unit. These uncompensated charges and hydrogen bond donors lead to a disordered network of Na⁺ ions as well as MeOH and H₂O molecules along the *b* axis. It is interesting to compare this arrangement with the iron binding site of the metalloprotein lactoferrin, which is known to reversibly bind two Fe^{III} ions concomitantly with two CO₃^{2−} groups by two equal mononuclear binding sites.^[17] A synergistic relationship between cation- and anion-binding has been established. The carbonate anion coordinated to the Fe^{III} ion is tightly fixed by five hydrogen bonds from the protein backbone. In this respect, the stabilization of CO₃^{2−} in **1** by hydrogen bonds and Na⁺ ions indicates that the oxygen rich environment of the dinuclear

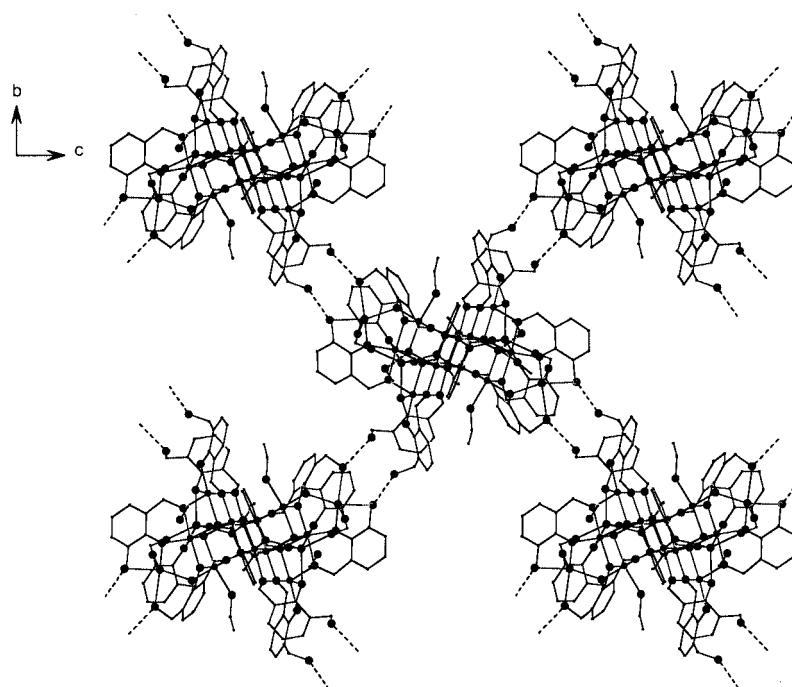


Figure 3. Projection down the *bc*-plane of the 2D network formed from interconnected $\text{Fe}_{10}\text{Na}_4$ complexes by intermolecular hydrogen bonds in crystals of **2**

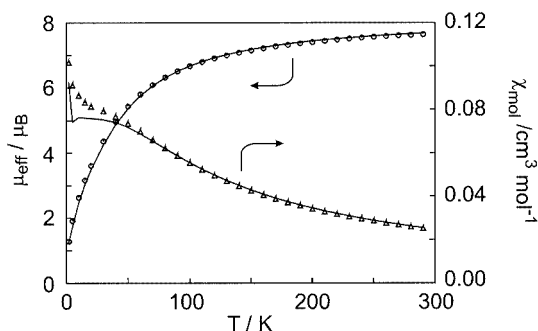


Figure 4. Temperature dependence of the effective magnetic moment, μ_{eff} , of **1'** at 1 T; the solid line is a fit of the experimental data using the spin-Hamiltonian given in the text with $J = -4.4 \text{ cm}^{-1}$, $g = 1.98$, and a paramagnetic impurity of same molecular mass of 4.1% ($S = 5/2$)

iron unit corroborated by the $\text{Na}^+/\text{MeOH}/\text{H}_2\text{O}$ network is perfectly suited for CO_3^{2-} binding. It may be speculated that this is the reason why, by use of MeOH as the solvent, **1** is formed rather than a high-nuclearity iron complex analogous to **2**.

Complex **2** possesses a central iron-oxygen core which may be regarded as a small fraction of the hydrous ferric oxide mineral lepidocrocite. This iron-oxygen core is surrounded by 12 HL^{2-} ligands. In the case of **2**, the uncompensated negative charges of the oxygen donors are saturated by incorporation of four Na^+ ions to give the neutral $\text{Fe}_{10}\text{Na}_4$ complex. The packing of **2** in the solid state is not governed by van der Waals forces. The presence of eight BzOH functions grouped in four pairs on the surface of **2**

leads to a regular hydrogen bonding pattern in a 2D array in the *bc*-plane. The only weakly bound solvent molecules evaporate very rapidly when the crystals are extracted from the mother liquor.

In summary, the coordination chemistry of the ligand 4-*tert*-butyl-2,6-bis(hydroxymethyl)phenol (H_3L) is different from its 2,6-bis(amino) and 2,6-bis(imino) derivatives. Several different coordination modes of H_3L were observed in compounds **1**, **2**, and **3**. The tendency of the OBz^- functions to bridge between metal centers and the availability of BzOH for hydrogen bonds leads to high nuclearity complexes and/or to intermolecular interactions in the solid state. The preparation of manganese complexes of H_3L with the possibility of interesting magnetic properties is currently under way.

Experimental Section

Syntheses: All manipulations were performed under aerobic conditions, using materials as received. 4-*tert*-butyl-2,6-bis(hydroxymethyl)phenol (H_3L) was prepared as described previously^[6a]

Safety Note: Although we have not encountered any problems, it has been noted that the reaction between perchlorate salts and organic ligands may lead to potentially explosive materials and must be performed with great care and appropriate precautions.

$\text{Na}_4(\text{HL})_4\text{Fe}^{\text{III}}_2(\text{CO}_3)_2 \cdot 8\text{MeOH} \cdot 2\text{H}_2\text{O}$ (1'**):** A stirred solution of 4-*tert*-butyl-2,6-bis(hydroxymethyl)phenol (400 mg, 1.90 mmol) in methanol (30 mL) was treated with $\text{Fe}^{\text{III}}(\text{ClO}_4)_3 \cdot 10\text{H}_2\text{O}$ (508 mg, 0.95 mmol) resulting in a deep blue solution. Addition of NaOH (380 mg, 9.51 mmol) caused a color change to dark red. The solu-

tion was heated at reflux for 4 h during which the color became light red, cooled to room temperature, and filtered. Slow evaporation of the solvent produced red crystals which were vacuum dried. Yield: 420 mg (63%). IR (KBr): $\tilde{\nu}$ = 3538, 2954, 2904, 2868, 1605, 1480, 1392, 1363, 1307, 1276, 1219, 1124, 1039, 1021 878, 832, 757, 690, 549 cm⁻¹. C₅₇H₁₀₀Fe₂Na₄O₂₅ (1389.06): calcd. C 49.29, H 7.26; found C 49.31, H 6.98.

[(HL)₁₂Fe^{III}₁₀Na₄(μ₄-O)₄(μ₃-OH)₂(dme)₂(EtOH)₂]-2dme·8EtOH (2): A stirred solution of 4-*tert*-butyl-2,6-bis(hydroxymethyl)phenol (300 mg, 1.43 mmol) in ethanol (10 mL) was treated with Fe^{III}(ClO₄)₃·10H₂O (389 mg, 0.73 mmol) resulting in the formation of a deep blue color. Addition of a solution of NaOH (214 mg, 5.35 mmol) in ethanol (10 mL) caused a color change to dark red. After stirring for 30 min, dme (3 mL) was added and the solution was filtered. Slow evaporation of the solvent produced red crystals which were vacuum dried. Yield: 160 mg (63%). IR (KBr): $\tilde{\nu}$ = 3424, 2954, 2867, 1624, 1606, 1540, 1480, 1393, 1363, 1306, 1275, 1220, 1122, 1038, 1022, 878, 833, 759, 617, 555 cm⁻¹. C₁₅₆H₂₂₆Fe₁₀Na₄O₄₈ (3519.91): calcd. C 53.23, H 6.47; found C 53.12, H 6.14.

Crystal Structure Determination: Data were collected with a Bruker AXS APEX diffractometer equipped with a rotating anode using Mo-*K*_α radiation (λ = 0.71073 Å). An empirical absorption correction was applied for **2** using SADABS.^[18] The structure was solved with SHELXS^[19] using direct methods and refined with SHELXL.^[20]

Single crystals of **2** rapidly desolvate when extracted from the mother liquor indicating the presence of weakly bound solvent molecules. The structure solution shows the well defined complex [(HL)₁₂Fe^{III}₁₀Na₄(μ₄-O)₄(μ₃-OH)₂(dme)₂(EtOH)₂] which could be refined unrestrained using anisotropic thermal parameters. These molecules are separated by solvent layers. Due to heavy disorder, the solvent positions are only poorly resolved and are estimated to consist of eight ethanol and two dme molecules per Fe₁₀Na₄ complex. Hydrogen atoms were added in calculated positions and no hydrogen positions were calculated for solvent molecules. Additional data collection and refinement details are listed in Table 2. CCDC-170255 contains the supplementary crystallographic data for compound **2**. These data can be obtained free of charge via www.ccdc.cam.ac.uk/conts/retrieving.html [or from the CCDC, 12 Union Road, Cambridge CB2 1EZ, UK; Fax: (internat.) +44 1223 336033; E-mail: deposit@ccdc.cam.ac.uk].

Other Measurements: Infrared spectra (400–4000 cm⁻¹) of solid samples were recorded with a Bruker Vector 22 spectrometer as KBr disks. Temperature-dependent magnetic susceptibilities of powdered samples in gelatin capsules were measured using a SQUID magnetometer (Quantum Design) at 1.0 T (2.0–300 K). For calculations of the molar magnetic susceptibility, χ_M , the measured susceptibilities were corrected for the diamagnetism of the sample holder and for the underlying diamagnetism of the sample by using tabulated Pascal's constants (1': $\chi_{dia} = -813 \times 10^{-6}$ cm³·mol⁻¹; 2: $\chi_{dia} = -1997 \times 10^{-6}$ cm³·mol⁻¹). ⁵⁷Fe Mössbauer spectra were recorded with an alternating constant-acceleration spectrometer. The minimal line-width was 0.24 mm·s⁻¹ full-width at half-height. The sample temperature was maintained in an Oxford Instruments Variox Cryostat. ⁵⁷Co/Rh was used as the radiation source. Isomer shifts were determined relative to α -iron at 300 K.

Electronic Supporting Information Available (see also footnote on the first page of this article): Graphical representations of the hydrogen

Table 2. Crystallographic data for **2**

	2
Habit	orange plates
Crystal size (mm)	0.45 × 0.14 × 0.06
Empirical formula	C ₁₈₀ H ₂₉₄ Fe ₁₀ Na ₄ O ₆₀
Molecular mass (amu)	4068.61
<i>a</i> (Å)	17.9317(4)
<i>b</i> (Å)	23.5919(4)
<i>c</i> (Å)	26.7758(5)
β (deg)	91.028(1)
<i>V</i> (Å ³)	11325.5(4)
Space group	<i>P</i> 2 ₁ / <i>c</i>
<i>Z</i>	2
μ (mm ⁻¹)	0.699
Absorption correction	multi-scan (SADABS)
<i>T</i> _{min} / <i>T</i> _{max}	0.744/0.956
2 θ Range (deg)	2.3–45
<i>T</i> (K)	153(2)
Measured data	49353
Unique data	14752
Observed [<i>I</i> > 2 σ (<i>I</i>)]	9881
<i>R</i> (observed) (%)	7.71, <i>R</i> _w = 24.10
<i>R</i> (all) (%)	10.88, <i>R</i> _w = 26.88
GOF	1.044
Number of variables	1062
Number of restraints	0
Res. electron density (e ⁻ Å ⁻³)	–0.783/1.316

bond between O2 and O11 in **2** and the packing of the iron-oxygen core in **2** have been deposited.

Acknowledgments

We thank Dr. E. Bill (Max-Planck-Institut für Bioanorganische Chemie, Mülheim) for susceptibility and Mössbauer measurements and valuable discussions. Prof. A. K. Powell (University Karlsruhe) is thanked for helpful discussions. T. G. gratefully acknowledges Professor F. E. Hahn for his generous support. This work was supported by the Fonds der Chemischen Industrie (Liebig-Stipendium for T. G.), the BMBF (Kooperationsbereich Neue Materialien), the Deutsche Forschungsgemeinschaft (Priority Program "Molecular Magnetism"), and the Dr. Otto Röhm Gedächtnisstiftung.

[1] A. K. Powell, *Structure and Bonding* **1997**, 88, 1–38 and references cited therein.

[2] [2a] A.-L. Barra, P. Debrunner, D. Gatteschi, Ch. E. Schulz, R. Sessoli, *Europhys. Lett.* **1996**, 35, 133–138. [2b] H. Oshio, N. Hoshino, T. Ito, *J. Am. Chem. Soc.* **2000**, 122, 12602–12603. [2c] A. L. Barra, A. Caneschi, A. Cornia, F. Fabrizi de Biani, D. Gatteschi, C. Sangregorio, R. Sessoli, L. Sorace, *J. Am. Chem. Soc.* **1999**, 121, 5302–5310.

[3] [3a] Fe₁₉/Fe₁₇: A. K. Powell, S. L. Heath, D. Gatteschi, L. Pardi, R. Sessoli, G. Spina, F. Del Giallo, F. Pieralli, *J. Am. Chem. Soc.* **1995**, 117, 2491–2502. [3b] Fe₁₄: J. Burger, P. Klüfers, *Angew. Chem.* **1997**, 109, 801–804; *Angew. Chem. Int. Ed. Engl.* **1997**, 36, 776–779. [3c] Fe₁₃: A. Bino, M. Ardon, D. Lee, B. Springler, S. J. Lippard, *J. Am. Chem. Soc.* **2002**, 124, 4578–4579. [3d] Fe₁₁: S. M. Gorun, G. C. Papaefthymiou, R. B. Frankel, S. J. Lippard, *J. Am. Chem. Soc.* **1987**, 109, 3337–3348. [3e] Fe₁₀: A. Caneschi, A. Cornia, A. C. Fabretti, D. Gatteschi, *Angew. Chem.* **1995**, 107, 2862–2864; *Angew.*

- Chem. Int. Ed. Engl.* **1995**, *34*, 2862–2864. ^[3f] Fe₁₀⁺: S. Asirvatham, M. A. Khan, K. M. Nicholas, *Inorg. Chem.* **2000**, *39*, 2006–2007. ^[3g] Fe₉: A. Bino, I. Shweky, S. Cohen, E. R. Bauminger, S. J. Lippard, *Inorg. Chem.* **1998**, *37*, 5168–5172. ^[3h] Fe₈: C. Delfs, D. Gatteschi, R. Sessoli, K. Wieghardt, D. Hanke, *Inorg. Chem.* **1993**, *32*, 3099–3103. ^[3i] Fe₈⁺: V. S. Nair, K. S. Hagen, *Inorg. Chem.* **1994**, *33*, 185–186. ^[3j] Fe₈⁺: I. Gautier-Luneau, C. Fouquard, C. Merle, J.-L. Pierre, D. Luneau, *J. Chem. Soc., Dalton Transactions* **2001**, 2127–2131.
- [4] M. Murugesu, C. E. Anson, A. K. Powell, *Chem. Commun.* **2002**, 1054–1055.
- [5] ^[5a] R. Robson, *Inorg. Nucl. Chem. Lett.* **1970**, *6*, 125–128. ^[5b] R. Robson, *Aust. J. Chem.* **1970**, *23*, 2217–2224. ^[5c] H. Okawa, S. Kida, *Bull. Chem. Soc. Jpn.* **1971**, *44*, 1172. ^[5d] A. J. Atkins, D. Black, R. L. Flinn, A. Martin-Becerra, A. J. Blake, L. Ruiz-Ramirez, W.-S. Li, M. Schröder, *Dalton Trans.* **2003**, 1730–1737 and references cited therein.
- [6] ^[6a] T. Glaser, T. Lügger, *Inorg. Chim. Acta* **2002**, *337*, 103–112. ^[6b] A. Rammel, F. Brisach, M. Henry, *J. Am. Chem. Soc.* **2001**, *123*, 5612–5613.
- [7] ^[7a] K. Hegetschweiler, H. Schmalke, H. M. Streit, W. Schneider, *Inorg. Chem.* **1990**, *29*, 3625–3627. ^[7b] A. Cornia, D. Gatteschi, K. Hegetschweiler, L. Hausherr-Primo, V. Gramlich, *Inorg. Chem.* **1996**, *35*, 4414–4419. ^[7c] R. W. Saalfrank, I. Bernt, E. Uller, F. Hampel, *Angew. Chem.* **1997**, *109*, 2596–2599; *Angew. Chem. Int. Ed. Engl.* **1997**, *36*, 2482–2485. ^[7d] O. Waldmann, R. Koch, S. Schromm, J. Schüle, P. Müller, I. Bernt, R. W. Saalfrank, R. Hampel, E. Baltes, *Inorg. Chem.* **2001**, *40*, 2986–2996. ^[7e] R. W. Saalfrank, I. Bernt, M. M. Chowdhry, F. Hampel, G. B. M. Vaughan, *Chem. Eur. J.* **2001**, *7*, 2765–2769.
- [8] ^[8a] R. E. P. Winpenny, *Adv. Inorg. Chem.* **2001**, *52*, 1–111. ^[8b] R. E. P. Winpenny, *Dalton Trans.* **2002**, 1–10.
- [9] ^[9a] E. K. Brechin, J. Yoo, M. Nakano, J. C. Huffmann, D. N. Hendrickson, G. Christou, *Chem. Commun.* **1999**, 783–784. ^[9b] C. Boskovic, W. Wernsdorfer, K. Folting, J. C. Huffmann, D. N. Hendrickson, G. Christou, *Inorg. Chem.* **2002**, *41*, 5107–5118.
- [10] ^[10a] B. P. Gaber, V. Miskowski, T. G. Spiro, *J. Am. Chem. Soc.* **1974**, *96*, 6868–6873. ^[10b] D. C.-T. Siu, A. M. Orville, J. D. Lipscomb, D. H. Ohlendorf, L. Que Jr., *Biochemistry* **1992**, *31*, 10443–10448. ^[10c] A. Mukherjee, M. McGlashen, T. G. Spiro, *J. Phys. Chem.* **1995**, *99*, 4912–4917.
- [11] **1**: Triclinic, $P\bar{1}$, $a = 13.204(2)$, $b = 9.924(2)$, $c = 30.102(2)$ Å, $\alpha = 90.0^\circ$, $\beta = 112.098(2)^\circ$, $\gamma = 90.0^\circ$, $V = 3654.4(3)$ Å³, $T = 123(2)$ K, $Z = 2$. The dinuclear complex (65% of total scattering power) obeys monoclinic symmetry ($P2_1/c$) with regards to the given cell constants. The Na⁺/MeOH/H₂O network (35% of total scattering power) forces a symmetry reduction ($P2_1/c \rightarrow P\bar{1}$; translationengleiche symmetry reduction of index t_2). Although the dinuclear complex refines well in $P\bar{1}$ in combination with the twin law
- $$\begin{pmatrix} \bar{1} & 0 & 0 \\ 0 & 1 & 0 \\ 0 & 0 & \bar{1} \end{pmatrix},$$
- the Na⁺/MeOH/H₂O network still exhibits disorder which precludes complete refinement.
- [12] ^[12a] D. L. Jameson, C.-J. Xie, D. N. Hendrickson, J. A. Potenza, H. J. Schugar, *J. Am. Chem. Soc.* **1987**, *109*, 740–746. ^[12b] S. Druke, K. Wieghardt, B. Nuber, J. Weiss, *Inorg. Chem.* **1989**, *28*, 1414–1417. ^[12c] N. Arulsamy, D. J. Hodgson, J. Glerup, *Inorg. Chim. Acta* **1993**, *209*, 61–69. ^[12d] N. Arulsamy, P. A. Goodson, D. J. Hodgson, J. Glerup, K. Michelsen, *Inorg. Chim. Acta* **1994**, *216*, 21–29. ^[12e] J. Glerup, K. Michelsen, N. Arulsamy, D. J. Hodgson, *Inorg. Chim. Acta* **1998**, *274*, 155–166. ^[12f] R. E. Norman, R. C. Holz, S. Menage, C. J. O'Connor, J. H. Zhang, L. Que Jr., *Inorg. Chem.* **1990**, *29*, 4629–4637. ^[12g] A. Nishida, A. Goto, T. Akamatsu, S. Ohba, T. Fujita, T. Toki, S. Okada, *Chem. Lett.* **1994**, 641–644. ^[12h] R. Hazell, K. B. Jensen, C. J. McKenzie, H. Toftlund, *J. Chem. Soc., Dalton Trans.* **1995**, 707–717.
- [13] N. Kitajima, S. Hikichi, M. Tanaka, Y. Moro-oka, *J. Am. Chem. Soc.* **1993**, *115*, 5496–5508.
- [14] ^[14a] A. L. Feig, S. J. Lippard, *Chem. Rev.* **1994**, *94*, 759–805. ^[14b] L. Que Jr., Y. Dong, *Acc. Chem. Res.* **1996**, *29*, 190–196. ^[14c] L. Que Jr., *J. Chem. Soc., Dalton Trans.* **1997**, 3933–3940.
- [15] ^[15a] B. F. Anderson, D. A. Buckingham, G. B. Robertson, J. Webb, K. S. Murray, P. E. Clark, *Nature* **1976**, *262*, 722–724. ^[15b] G. M. Grant, M. J. Knapp, J. C. Huffman, D. N. Hendrickson, G. Christou, *Chem. Commun.* **1998**, 1753–1754. ^[15c] G. M. Grant, M. J. Knapp, W. E. Streib, J. C. Huffman, D. N. Hendrickson, G. Christou, *Inorg. Chem.* **1998**, *37*, 6065–6070. ^[15d] A. Horn Jr., A. Neves, I. Vencato, V. Drago, C. Zucco, R. Werner, W. Haase, *J. Braz. Chem. Soc.* **2000**, *11*, 7–10. ^[15e] M. Scarpellini, A. Neves, A. J. Bortoluzzi, I. Vencato, V. Drago, W. Ortiz, C. Zucco, *J. Chem. Soc., Dalton Trans.* **2001**, 2616–2623.
- [16] The JULIUS routine was used for spin Hamiltonian simulations of the data (C. Krebs, E. Bill, F. Birkelbach, V. Stammel, unpublished results). For the calculation of the magnetic susceptibility of the paramagnetic impurity JULIUS uses the molar mass of the main component. Thus the obtained value of 4.1% for the paramagnetic impurity is far overestimated if a mononuclear Fe^{III} species is anticipated.
- [17] ^[17a] E. N. Baker, S. V. Rumball, B. F. Anderson, *Trends Biochem. Sci.* **1987**, *12*, 350–354. ^[17b] E. N. Baker, *Adv. Inorg. Chem.* **1994**, *41*, 389–463.
- [18] SMART, Bruker AXS, **2000**.
- [19] SHELXS-97, G. M. Sheldrick, *Acta Crystallogr., Sect. A* **1990**, *46*, 467–473.
- [20] SHELXL-97, G. M. Sheldrick, University of Göttingen, **1997**.

Received August 18, 2003

Early View Article

Published Online April 7, 2004